

A bimodal volcanic–plutonic system: the Zarembo Island extrusive suite and the Burnett Inlet intrusive complex

Jennifer Lindline, William A. Crawford, and Maria Luisa Crawford

Abstract: The Zarembo Island volcanic rocks and the Burnett Inlet plutonic complex in central southeastern Alaska were investigated to determine if they are genetically related. The Zarembo Island volcanic suite consists of basalt, andesite, and rhyolite lava flows, which exhibit features that suggest simultaneous eruptions of mafic and felsic lavas. Five kilometres to the southeast, the broadly layered Burnett Inlet plutonic complex consists of gabbro–diorite and granite plutons that also show characteristics of contemporaneous mafic and felsic magmatism. These bimodal volcanic and plutonic rocks are similar in age, ranging from 18.5 to 21.5 Ma. Both suites show a gap in silica concentration between 60 and 65 wt.% and have similar major, trace, and rare-earth element composition. Both suites also show igneous layering, either as interlayered basalt and rhyolite flows or as alternating gabbro and granite sheets. Additionally, both groups contain magma mingling and mixing textures, including mafic enclaves in felsic members and quartz xenocrysts rimmed by clinopyroxene in enclaves. These characteristics suggest that the Burnett Inlet intrusive complex and the Zarembo Island volcanic suite represent an eroded, shallow-level plutonic center and its eruptive cover. The style of volcanism and the bimodal nature of magmatism suggest that igneous activity occurred during crustal extension and thinning that accompanied strike-slip tectonic motion in southeastern Alaska during the Tertiary. The volcanic–plutonic rock associations now exposed at the surface indicate that at least 7° of post-20 Ma crustal tilting has affected the region and can help to explain aberrant paleomagnetic poles in mid-Cretaceous intrusions of the Cordillera Coast belt.

Résumé : Les roches volcaniques de l'île de Zarembo et celles du complexe plutonique du bras de Burnett dans le sud-est central de l'Alaska ont été étudiées afin de déterminer si elles sont génétiquement reliées. La suite volcanique de l'île de Zarembo comprend du basalte, de l'andésite et des coulées de lave rhyolitique qui montrent des caractéristiques suggérant des éruptions simultanées de laves mafiques et felsiques. À cinq kilomètres au sud-est, le complexe du bras de Burnett, largement lité, comprend des plutons de gabbro–diorite et de granite qui montrent aussi des caractéristiques de magmatisme mafique et felsique contemporain. Ces roches bimodales, volcaniques et plutoniques, ont des âges semblables, variant de 18,5 – 21,5 Ma. Les deux suites montrent un manque, variant entre 60 et 65 pour cent (poids), dans la concentration en silice et elles ont des compositions semblables en ce qui concerne les éléments majeurs, en traces et de terres rares. Les deux suites montrent aussi du litage igné soit comme des écoulements interlités de basalte et de rhyolite ou en feuillets alternés de gabbro et de granite. De plus, les deux groupes contiennent des textures de malaxage et de mélange incluant des enclaves mafiques dans les membres felsiques et des xénocristaux de quartz bordés de clinopyroxène dans des enclaves. Ces caractéristiques suggèrent que le complexe intrusif du bras de Burnett et la suite volcanique de l'île de Zarembo représentent un centre plutonique, érodé et de faible profondeur, avec son couvert de roche éruptive. Le style de volcanisme et la nature bimodale du magmatisme suggèrent de l'activité ignée au cours de l'extension et l'amincissement de la croûte qui accompagnait, au Tertiaire, le mouvement tectonique coulissant dans le sud-est de l'Alaska. Les associations de roches volcaniques–plutoniques affleurant maintenant à la surface indiquent qu'après 20 Ma un basculement d'au moins 7° a affecté la région; cela peut aider à expliquer les pôles paléomagnétiques aberrants dans les intrusions, au Crétacé moyen, de la ceinture de la cordillère côtière.

[Traduit par la Rédaction]

Introduction

The volcanic rocks on Zarembo Island are one of several Tertiary to Quaternary (?) volcanic assemblages (Brew et al.

1984; Douglass et al. 1989) that occur along the coast of southeastern Alaska. These volcanic rocks and the Burnett Inlet plutonic complex on nearby Etolin and Deer islands are part of the 170-km long Middle Miocene Kuiu–Etolin Igneous

Received 28 July 2003. Accepted 4 February 2004. Published on the NRC Research Press Web site at <http://cjcs.nrc.ca> on 31 March 2004.

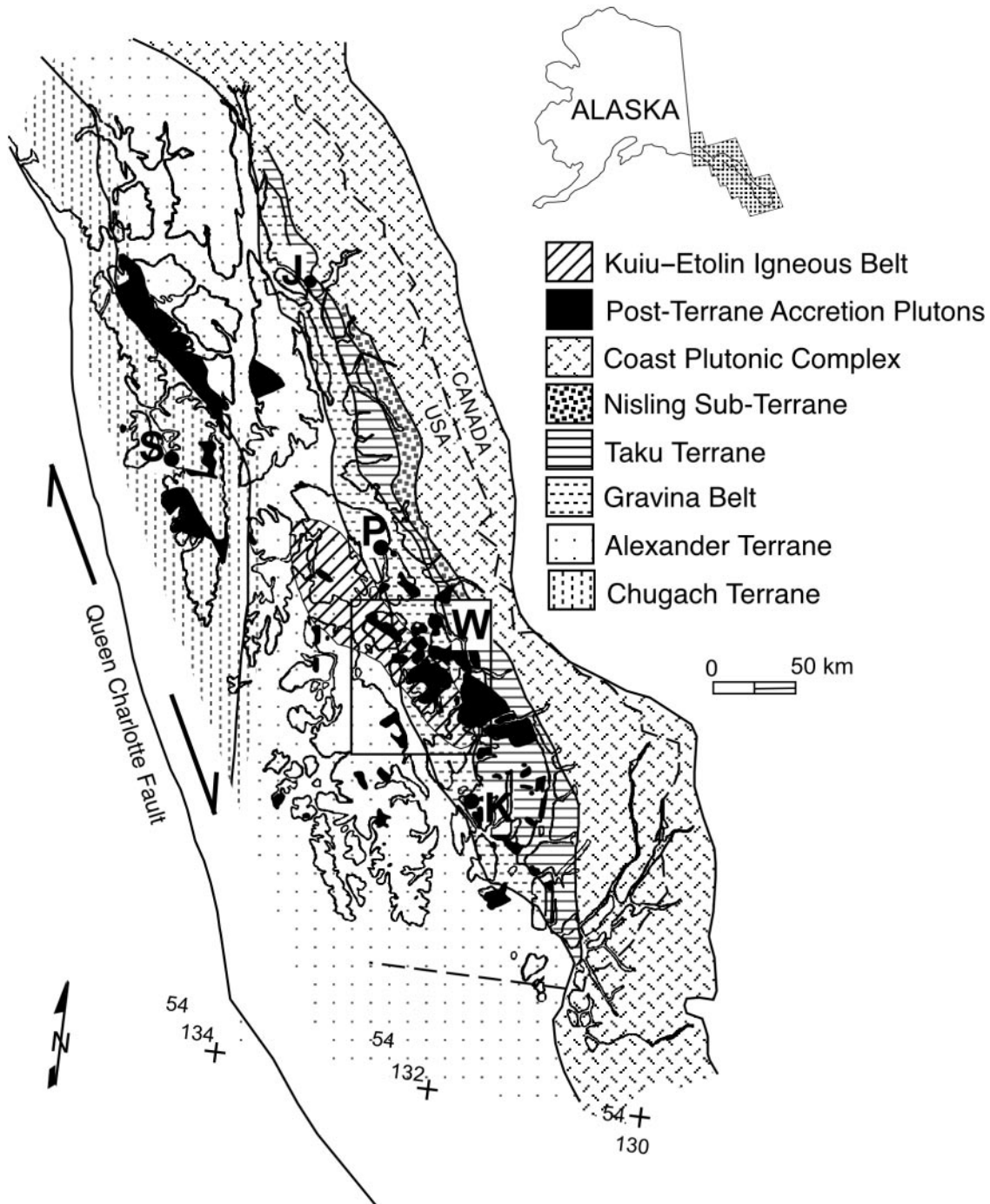
Paper handled by Associate Editor J.D. Greenough.

J. Lindline.¹ Natural Sciences Department - Environmental Geology Program, New Mexico Highlands University, Las Vegas, NM 87701, USA.

W.A. Crawford and M.L. Crawford. Geology Department, Bryn Mawr College, Bryn Mawr, PA 19010, USA.

¹Corresponding author (e-mail: lindlinej@nmhu.edu).

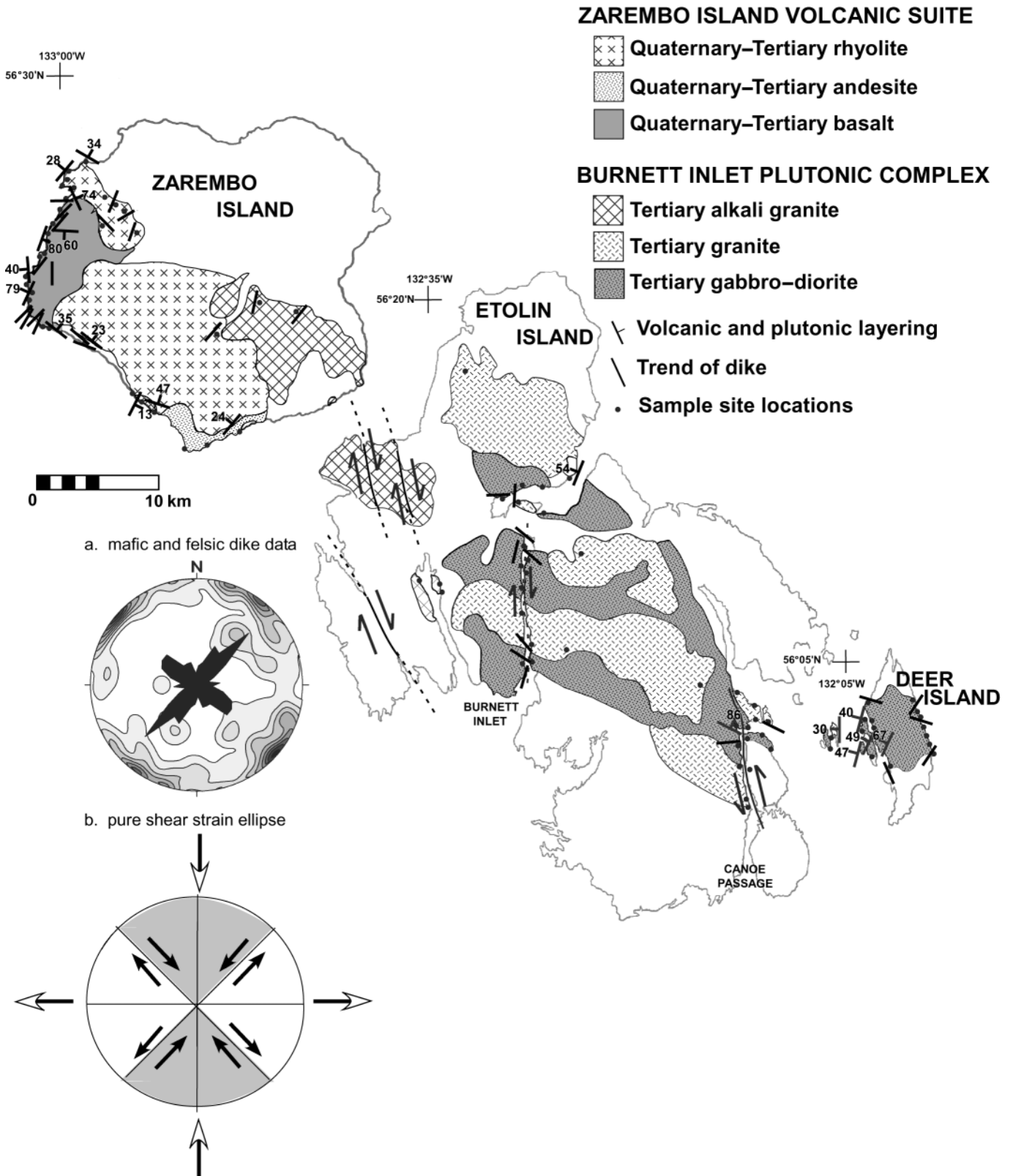
Fig. 1. Map of lithotectonic units in southeastern Alaska after Wheeler et al. (1991) showing the location and extent of the Kuiu–Etolin Igneous Belt (Brew 1994; Brew and Morrell 1983; Brew et al. 1984). Box encloses study area shown in Fig. 2. Larger towns and features: K, Ketchikan; W, Wrangell; P, Petersburg; S, Sitka; J, Juneau.



Belt (Brew et al. 1979, 1981; Brew and Morrell 1983) (Figs. 1, 2). The Kuiu–Etolin Igneous Belt is a discontinuous tract of predominantly silicic volcanic and plutonic rocks. The genetic relationship among specific volcanic and plutonic rocks in the province was not previously established. In this study, we investigated the Zarembo Island volcanic rocks and the Burnett Inlet plutonic complex to determine if a genetic relationship exists between the two rock groups and if such a relationship could assist in understanding the magmatic

and tectonic history of the region. Our results show that the Zarembo Island volcanic suite and the Burnett Inlet plutonic complex display a number of shared features suggesting that the two are cogenetic: (i) both include felsic and mafic lithologies with few intermediate rock types; (ii) felsic members (rhyolite flows, granite intrusions, and felsic dikes) contain mafic magmatic enclaves; (iii) both assemblages show a gap in silica concentration between 60 and 65 wt.%; (iv) both have similar ranges in trace element chemistry and nearly

Fig. 2. Simplified geological map of the study area after Brew et al. (1984). Map shows all field sites (●) and representative structural data. (a) Lower hemisphere projection of pole-density data and composite rose diagram (center of circle) showing the orientations of dikes throughout the study area. $N = 138$. (b) Pure shear strain ellipse showing major stress field (open arrows) that corresponds with highly oblique collision of the Pacific Plate with North America between 10 and 19 Ma and conjugate NW-NE shear fractures (solid arrows). Notice that the shear fractures parallel the major dike sets.



identical chondrite-normalized rare-earth element patterns; and (v) both have geochemical signatures suggestive of within-plate magmatism.

In addition to the lithological and geochemical similarities just listed, both the Zarembo Island volcanic suite and Burnett Inlet plutonic complex show igneous layering. The Zarembo Island volcanic suite exhibits interlayered basalt, andesite, and rhyolite flows, while the Burnett Inlet plutonic complex shows alternating granite and gabbro sheets. Both the volcanic and plutonic rocks contain magma mingling and magma mixing textures, such as mafic enclaves in felsic members and quartz xenocrysts rimmed by clinopyroxene in mafic members. Commingling of chemically distinct magmas has been documented extensively in both plutonic (Wiebe 1974, 1988, 1993a, 1993b; Furman and Spera 1985; Frost and Mahood 1987; Zorpi et al. 1989) and volcanic (Eichelberger 1980; Bacon and Metz 1984; Bacon 1986) systems. The bimodal Zarembo Island – Burnett Inlet volcanic–plutonic system is a rare geologic exposure that reveals, from southeast to northwest, both the intrusive and eruptive products of mafic and felsic magma interactions.

Regional geology

The geologic history of southeastern Alaska from the middle Jurassic through the Eocene was marked by the accretion of tectonostratigraphic terranes to western North America (Coney et al. 1980; Jones et al. 1981; Monger et al. 1982; Coney and Jones 1985) (Fig. 1). Numerous 100–90 million year old (Ma) calc-alkaline bodies of foliated garnet- and epidote-bearing plagioclase-porphyratic quartz diorite, tonalite, and granodiorite occur throughout the region. These intermediate composition rocks represent the deeply eroded remains of an Andean-type or continental margin arc formed in response to subduction of oceanic crust during the mid-Cretaceous. Subsequently, the Coast Mountains Batholith was emplaced from latest Cretaceous to Eocene (75–50 Ma; Gehrels et al. 1991). During the Late Eocene (43 Ma), convergence of the Pacific and North American plates changed to the present dominantly dextral strike-slip motion (Engelbreton et al. 1985; Stock and Molnar 1988; Lonsdale 1988). The reconstructions of Stock and Molnar (1988) indicate that since 43 Ma, strike-slip motion was interrupted by intervals of highly oblique convergence and divergence. Following an ~35 Ma lull in igneous activity, post-terranic accretion magmatism generated the Middle Miocene Kuiu–Etolin Igneous Belt, a discontinuous tract of volcanic and plutonic rocks that cuts across the tectonostratigraphic terrane boundaries established during the Mesozoic accretionary events.

Geology of the Zarembo Island volcanic suite and the Burnett Inlet intrusive complex

The volcanic rocks

Contact relations

Quaternary to upper Tertiary volcanic rocks extend from Zarembo Island northward to Kuiu Island. Several whole-rock andesite and rhyolite samples from Kupreanof Island (6 km northwest of Zarembo Island) were dated via the K/Ar method at 20.4 ± 0.6 to 21.5 ± 0.6 Ma (Douglass et al. 1989). This

study focused on field mapping and sampling on Zarembo Island, where reconnaissance mapping by the United States Geological Survey showed that the western side of the island contains a range of volcanic lithologies, including rhyolite, andesite, and basalt flows and various pyroclastic rocks (Brew et al. 1984; Karl et al. 1999). In many places, the rhyolite, andesite, and basalt flows are interlayered, indicating simultaneous or alternating eruption. The area is extensively cut by faults and numerous mafic and felsic dikes. This, the discontinuous nature of the coastline exposures and lack of inland outcrops made it impossible to establish a volcanic stratigraphy. The Tertiary Kootznahoo Formation, a light greenish gray, medium to coarse grained, lithofeldspathic fluvial sandstone is the only unit noted to stratigraphically interdigitate with mafic and felsic flows (Karl et al. 1999).

Description of the rocks

Much of the west and southwest of Zarembo Island is underlain by rhyolite. At some localities, the rhyolite is aphanitic; at others, it contains medium-sized quartz and potassium feldspar phenocrysts. The aphyric and flow-banded subunits are relatively uniform and range from 0.5 to 2.0 m in thickness. The aphyric rhyolite often demonstrates flow banding, though massive flows are equally abundant. The porphyritic rhyolite is massive and commonly exhibits extensive conchoidal fracturing. Rarely, but conspicuously, the rhyolite contains small, centimetre-sized mafic inclusions with very fine-grained igneous textures. Though some of the inclusions may represent solid clasts of basalts that were incorporated into the rhyolite during flow, those having rounded shapes and lobate boundaries are interpreted as mafic magmatic enclaves. Particularly, those mafic inclusions with a preferred orientation are interpreted to have been incorporated into the rhyolite and transported as plastic droplets of basalt (Fig. 3).

The andesite is a massive homogeneous unit with an aphanitic to fine-grained plagioclase–clinopyroxene intergranular texture. Some outcrops contain 1.0 mm round quartz crystals.

Rarely, the andesite exhibits flow banding. Metre-wide andesite columns were noted on southern Zarembo Island (Fig. 4). Several 3.0–5.0 m diameter vents were identified by cylindrical openings surrounded by radial joints and outward extending subhorizontal fractures resembling flow layering. Agglomerate, characterized by 1.0–15.0 cm angular to bulbous inclusions in a similar colored and textured aphanitic matrix, was noted in and around these areas.

The basalt unit is layered to massive with planar fracturing sub parallel to the surface. Where layered, the basalt flows are usually subhorizontal, 1.0–2.0 m in thickness, and underlain by a pyroclastic layer (Fig. 5). The basalt is aphanitic to fine-grained equigranular showing a plagioclase–pyroxene intergranular texture. Some basalt has plagioclase \pm clinopyroxene phenocrysts in a plagioclase-rich groundmass showing trachytic flow alignment. A few samples contain 1.0 mm pyrite cubes. Interstitial minerals include augite, orthopyroxene, and Fe–Ti oxides. The basalt is commonly vesicular and amygdaloidal. Vesicles are circular to oval in shape and range from 0.5–3.0 cm in diameter. The number and size of vesicles decrease downwards from the surface of the flow. Amygdaloidal minerals include epidote, calcite, and banded quartz. Two splatter zones were noted that show characteristics similar to those noted in the andesite vents.

Fig. 3. Mafic magmatic enclaves in flow-banded rhyolite, western Zarembo Island. The ovoid shape and preferred orientation of the inclusions suggest that the mafic enclaves were transported as plastic droplets of magma in the rhyolite flow. White specks on the outcrop are barnacles. Hammer for scale.



Fig. 4. Metre-wide andesite columns at Macnamara Point, southern Zarembo Island. The andesite layering is shallowly dipping to the northeast.



Fig. 5. Outcrop view of subhorizontal volcanic layering, Zarembo Island. The very fine-grained fragmental lower unit is rich in clay and interpreted as an ash-fall deposit. The upper massive unit is a basalt flow. Hammer for scale.



They consist of abundant agglomerate — black, very fine-grained volcanic debris with bulbous to blocky centimeter-sized inclusions similar to the host matrix.

Felsic pyroclastic layers typically occur beneath basalt or andesite flow layers. The felsite exhibits a felty surface, friable texture, and heterogeneous lithology (Fig. 5). Its matrix is commonly layered on the microscale, and contains a variety of inclusions, including basalt clasts and quartz ovoids ranging from 1.0–3.0 mm in diameter. The unit also contains centimetre-sized rough-textured ovoids having pitted surfaces that resemble pumice clasts in an ash and glass matrix. Some inclusions appear as 0.5 cm-sized black objects that are round in one aspect and oblong in another resembling volcanic fiamme. Other inclusions in the felsite are black, dull-lustered, round, pea-sized inclusions that are interpreted as devitrified spherulites. The spherulites are pale green in thin section, altered to a mixture of chlorite and clay minerals. The green hue of the felsite suggests subgreenschist-facies metamorphism and possible hydration of the glassy matrix to a chlorite-dominant assemblage.

Massive outcrops of debris-flow deposits (lahar) occur as metre-thick units interlayered with the volcanic flows or, more commonly, as massive decimetre-thick discontinuous exposures. These rocks are unsorted, clast-supported debris flows containing a variety of gravel- to boulder-sized rock fragments of varying lithologies including basalt, flow-banded rhyolite, andesite, spherulite-bearing felsite, welded tuff, and obsidian.

Plutonic rocks

Contact relations

The Burnett Inlet igneous complex, located on eastern Zarembo Island, Etolin and Deer islands (Fig. 2), is broadly layered and consists of three main units: gabbro–diorite, granite, and alkali granite. K/Ar dating of hornblende and biotite separates yielded ages of 18.5 ± 0.6 Ma (alkali granite), 19.9 ± 0.6 to 21.5 ± 0.9 Ma (granite), and 19.3 ± 0.6 to 21.4 ± 0.6 Ma (gabbro–diorite) (Douglass et al. 1989). Lindline et al. (2000) calculated a 22.47 ± 2.1 Ma crystallization age from whole-rock Rb–Sr isotope data for seven felsic rocks from the Burnett Inlet plutonic complex. The gabbro and granite magmas intruded fine-grained biotite-grade schist derived from the marine flysch sediments and interlayered volcanic rocks of the Jurassic–Cretaceous aged Gravina-Nutzotin belt Seymour Canal Formation (Berg et al. 1972; Brew et al. 1984). Gerdes (1988) estimated emplacement pressures between 2.1 and 2.3 kbars (1 kbar = 100 MPa) based on geobarometric calculations from a cordierite-bearing biotite schist on southern Deer Island. Contacts with the metamorphic rocks are straight, sharp, and discordant. The map patterns, constructed from shoreline and mountain top exposures, are very irregular in shape. The alkali granite outcrops predominantly on eastern Zarembo Island and northwestern Etolin Islands, while the gabbro–diorite outcrops on southern Etolin and Deer islands. Aeromagnetic mapping (Saltus and Simmons 1997) shows a magnetic high under central Deer Island that extends to the

Fig. 6. Mafic magmatic inclusions in granite, western Deer Island. Notice the fine-grained and crenulated enclave margin that indicates a magmatic origin.



east under Cleveland Peninsula suggesting that additional gabbro–diorite intruded the Bell Island pluton (a non-magnetic body).

Description of the rocks

The alkali granite is fine- to coarse-grained hypersolvus granite containing potassium feldspar with a well-developed perthitic texture and lacking plagioclase feldspar as separate grains. The granite also contains miarolitic cavities and graphic intergrowths. The rocks are generally allotriomorphic and equigranular to seriate with grain size ranging from medium to coarse. Modal analyses indicate that compositions include both alkali granite and alkali quartz syenite according to the International Union of Geological Sciences (IUGS) classification (Hunt 1984; Lindline et al. 2000). The feldspar in the granite is predominantly perthite, with minor amounts of either plagioclase or potassium feldspar as separate phases. Brown biotite and brown hornblende are common mafic minerals (<5 modal %) with rare sodic amphibole, iron-rich pyroxene, and iron-rich olivine. The granite unit grossly resembles the alkali granite but has a higher plagioclase content. Based on modes, the rocks are classified as granite, quartz syenite, and alkali quartz syenite. This unit also contains perthitic textures and graphic intergrowths, though both are much less extensively developed than in the alkali granite. The mafic phases include brown biotite and green hornblende, both partially altered to chlorite. Accessory titanite, zircon, and apatite as well as secondary epidote occur locally.

Both the granite and alkali granite are massive and homogeneous, except for the local presence of mafic inclusions or enclaves. Enclave margins are typically sharp and very fine-

grained; the enclave–granite contact in many areas is conspicuously crenulate (Figs. 6, 7), a feature frequently observed at liquid–liquid interfaces. The enclaves are, therefore, interpreted as blobs of commingled mafic magma. Though rare in most granite outcrops, enclaves locally make up 50% of the rock. They show a wide range of sizes and a variety of shapes from small globules (1 cm diameter) to large rafts. Enclaves are predominantly round to oblong, but may be pillowform, blocky, or highly irregular. Figure 7 shows a cliffside exposure of commingled mafic and felsic magma. In this and several other places around Deer Island, the mafic material form randomly oriented metre-sized rafts. The rafts all have one flat and smooth side and another flat but highly irregular side. The granite adjacent to the enclaves, as well as in enclave-absent outcrops, may contain mafic mineral clots, suggesting disaggregation and dispersion of enclaves throughout the pluton (Fig. 8). All enclaves display igneous microtextures; rarely, some enclaves contain quartz xenocrysts with green hornblende mantles.

The gabbro–diorite consists of plagioclase, clinopyroxene, orthopyroxene, hornblende, biotite, olivine, apatite ± quartz ± potassium feldspar. Modal compositions are predominantly olivine gabbro, hornblende gabbro, diorite, and quartz diorite, with lesser quartz monzonite and quartz monzodiorite (Lindline et al. 2000). The gabbro–diorite unit typically displays a massive medium- to coarse-grained subhedral equigranular texture. Clinopyroxene is ubiquitous and is often partly replaced by biotite and hornblende.

The gabbro–diorite unit includes interlayered mafic and granitic members. In the southeast area of the complex on and just west of Deer Island (Fig. 2), weak mineral layering

Fig. 7. Chaotic assemblage of mafic rafts in granite noted in cliff exposures, Deer Island. Each raft has a smooth side that is interpreted as the upper side of a mafic flow, as well as a sutured edge, which is interpreted as the base of a mafic flow veined by granitic material. The random orientation of the rafts indicates that the granite was mobilized after injection of one or more mafic layers, disrupting the mafic–felsic layering.

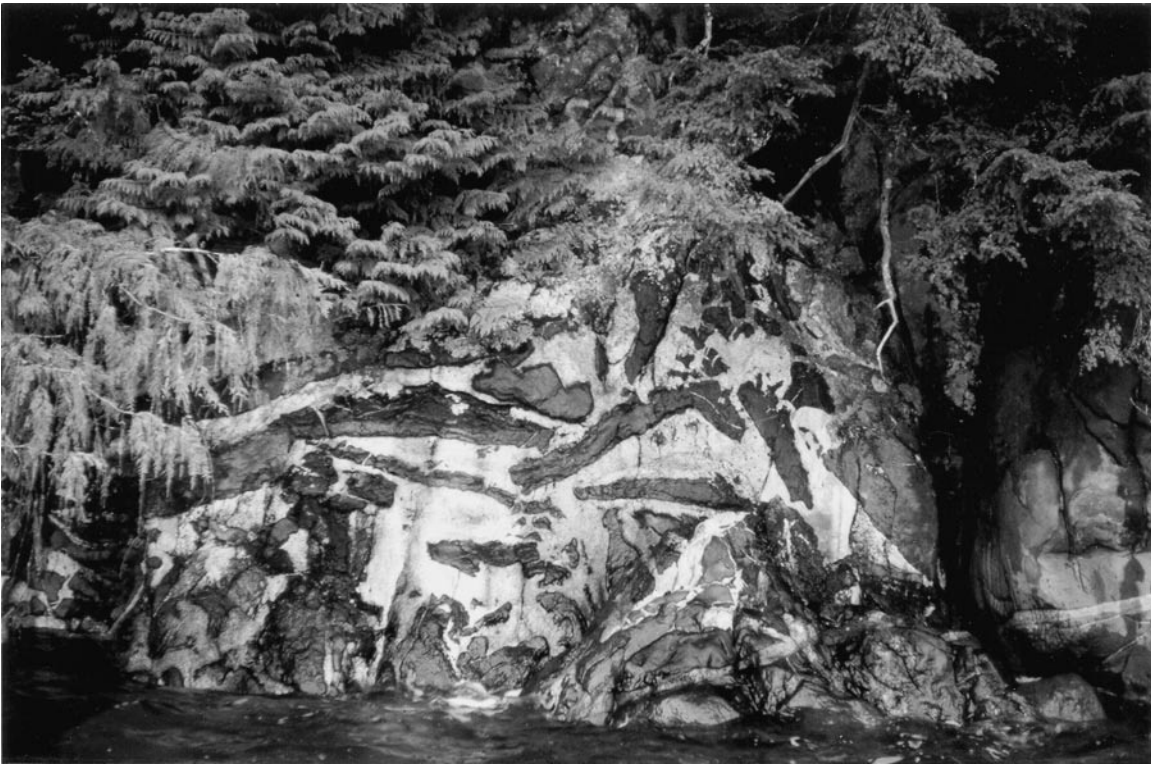


Fig. 8. Granite with mafic mineral clots, central Etolin Island. We interpret these mafic mineral clusters as mafic magmatic droplets that were disaggregated and dispersed throughout the pluton.



Fig. 9. Dipping intramagmatic mafic and felsic sheets, western Deer Island. The base of one mafic sheet (left) and the top of another sheet (right). Note the load cast development in the upper right area and granitic vein penetrating the mafic material to the right of scale.



and alternating mafic and felsic sheets in the gabbro–diorite (Fig. 9) dip west-northwest beneath the granite. Mafic sheets range from 1.0 to 5.0 m in thickness. A number of unusual features occur along the base of these units, including load casts, ball and pillow structures, and felsic veins (Figs. 9–11). The load casts appear as convex-downward lobes of mafic material extending into the granite. Randomly spaced, globular, mafic pillow-like structures range in size from small and nearly equant (5.0 cm by 5.0 cm) to large and elongate (1.0 m by 5.0 m). The pillows occur as discrete enclaves in granite or as globules connected to the main mafic sheet. Margins of the mafic bodies against the felsic matrix are sharp and fine-grained or quenched. At some granite–mafic magma interfaces, veins of granite extend into the gabbro unit for several centimetres. The matrix between the mafic pillows is most commonly homogeneous, coarse-grained granite and granodiorite. The amount of matrix material between enclaves varies, ranging from < 1.0 to 10.0 cm. In some zones of enclave accumulation, there is little to no matrix between the enclaves (Fig. 12). In other areas, the enclaves are matrix supported, with more than 5.0 cm of matrix material separating the mafic pillowed bodies (Fig. 13).

Mafic and felsic dikes

Numerous northeast- and northwest-trending mafic and felsic dikes crosscut the volcanic suite and plutonic complex, as well as neighboring rocks. Radiometric ages are not available for the dikes. The dikes range from 10.0 cm to 3.0 m in width; most are vertical or nearly vertical, though

there are a number of dikes with moderate dips. Many of the mafic and felsic dikes form composite or sheeted complexes. In the composite dikes, contacts are sharp yet lobate and serrated suggesting the mafic and felsic magmas were coeval. Mafic and felsic dikes alternate along much of the Zarembo Island shoreline. The felsic dikes display a tabular, flaggy weathering and are more easily eroded than their host rock. As a result, they may be more abundant than suggested by casual inspection in the field.

The mafic dikes are typically plagioclase ± clinopyroxene porphyritic in a plagioclase-rich matrix. Plagioclase is present as single phenocrysts, as glomerocrysts, and as framework microlites typically showing trachytic flow alignment. The matrix also includes intergranular orthopyroxene, augite, olivine, and magnetite and interstitial biotite, hornblende and quartz. Apatite is present as an accessory phase and chlorite as a mafic mineral alteration product. Several samples contain millimetre-sized quartz ovoids with thin continuous pyroxene mantles. The felsic dikes are aphanitic or porphyritic with potassium feldspar and quartz phenocrysts. Phenocrysts range from several millimetres up to 2.0 cm in size and are randomly oriented. The potassium feldspar phenocrysts are euhedral and occur as single crystals and as glomerocrysts. Quartz phenocrysts are always anhedral; they are typically round or irregular shaped and have a thin continuous pyroxene mantle. A number of felsic dikes contain mafic enclaves. They are 2.0 to 10.0 cm in size and rounded to teardrop-shaped with irregular, lobate boundaries. They are rarely isolated, but occur in clusters making up ~20% of the outcrop. Though not

Fig. 10. Connected ball and pillow structures at the base of a mafic layer, western Deer Island. These structures formed by foundering and breakup of semiconsolidated mafic material due to density instabilities in the underlying silicic crystal mush. Arrows point to leucocratic granitic veins that represent intercumulus liquid filter-pressed from within the granite. Dashed arrow points to the variably contaminated disconnected top of a teardrop shaped felsic diapir.

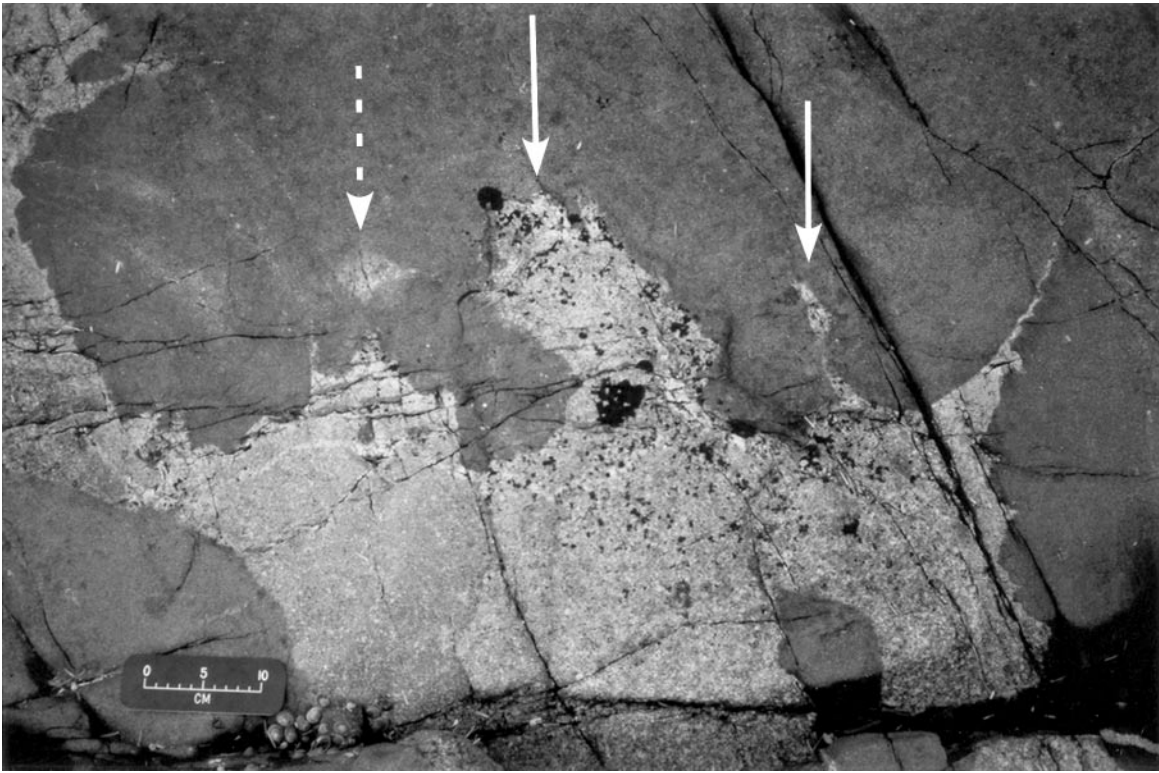


Fig. 11. Apparent base of a mafic sheet along tree-lined coastal exposure, western Deer Island. Note well-developed ball and pillow structures in mafic material.



Fig. 12. Densely packed mafic magmatic enclaves, Burnett Inlet.

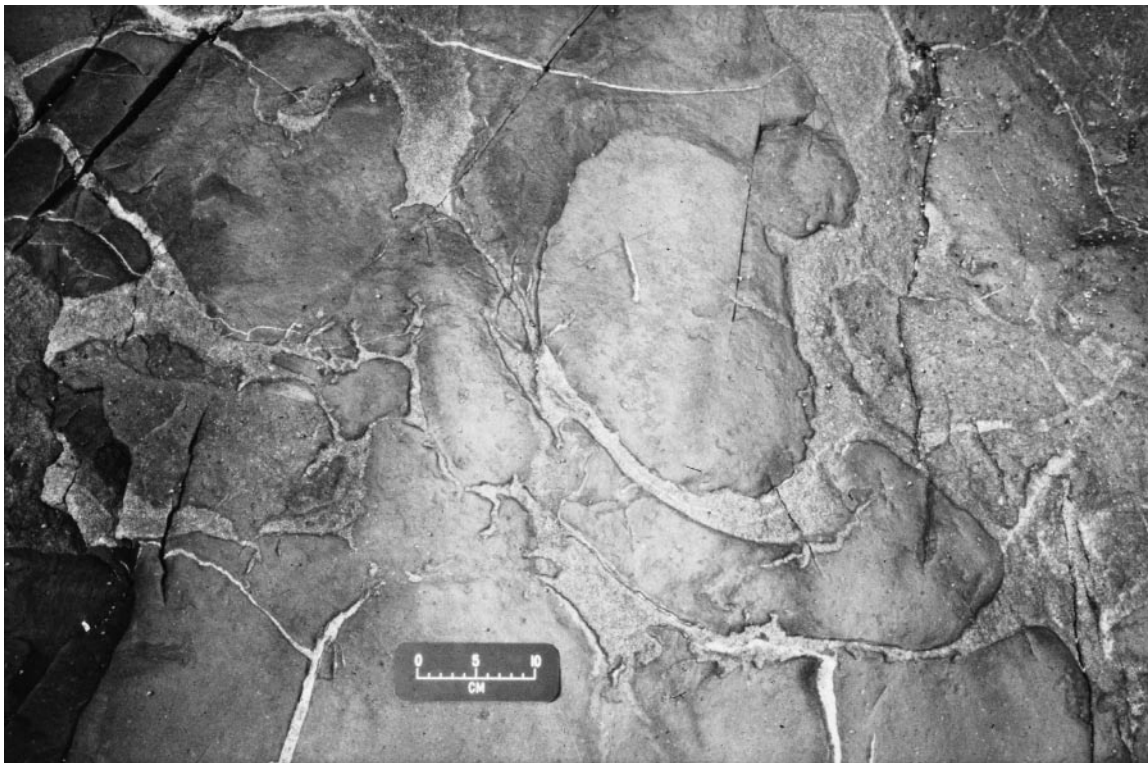


Fig. 13. Coastline exposure of granite–basalt commingling zone, Niblack Islands. The irregular volumes of host granite and variable mafic enclave shapes and sizes suggest that the granite and mafic magmas commingled as the mafic magma rose through a granitic crystal mush.



studied petrographically, the size, shape, and dimension of the mafic enclaves suggest that these, like the mafic inclusions in the rhyolite and granite, are magmatic in origin.

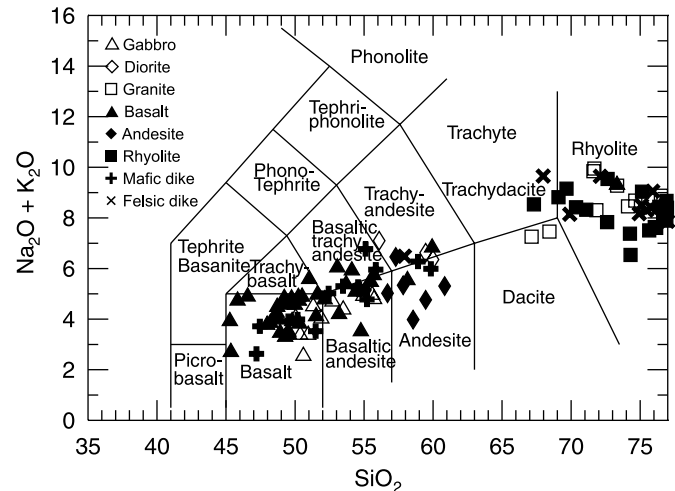
Geochemical comparisons

Seventeen plutonic rocks, 10 volcanic rocks, and 11 dike rocks were analyzed for major, trace, and rare-earth elements (REE) (Table 1). Major element analysis of underscored samples was conducted by direct current plasma atomic emission spectrometry – atomic emission spectrometry (DCP–AES) by Lindline at Bryn Mawr College, Pennsylvania, using the methods of Feigenson and Carr (1985). Trace and rare-earth element analysis of underscored samples was conducted by inductively coupled plasma mass spectrometry (ICP–MS) at Union College, New York. Replicate analyses of rock standards indicate a precision of $\pm 2\%$ for major elements and $\pm 5\%$ for trace elements. All other analyses were conducted by ICP–MS by Activation Laboratories, Ltd., Ontario, Canada with a precision of $\pm 2\%$ – 5% for major elements and $\pm 5\%$ – 10% for trace elements. The major element chemistry of some of the basalts and mafic dikes shows high loss on ignition values, signifying hydrothermal alteration. The chemical analyses were, therefore, normalized to a volatile-free basis on the major element variation diagrams to correct for the effects of variable hydration. Additional major element data for Zarembo Island volcanic rocks were taken from United States Geological Survey Open File Report 89-527 (Douglass et al. 1989) and added to the major element plots.

The volcanic and plutonic rocks span a broad range of silica with a distinct gap between 60 and 65 wt.% SiO_2 (Fig. 14). The rocks are subalkaline to slightly alkaline according to the definitions of Irvine and Baragar (1971). Within the separate mafic and felsic rock groups, major, trace, and REE compositions of volcanic, plutonic, and dike rocks are similar (Figs. 15–17). Most felsic rock samples have between 70 and 77 wt.% SiO_2 . They span a wide range in Al_2O_3 , Na_2O , K_2O , Rb, and Ba contents. The felsic rocks also show broad but overlapping ranges in compatible–incompatible trace element ratios (Ba/Nb and La/Sm) and a small range in REE concentrations and patterns (Fig. 16). They are 15 to 110 times enriched in the light REE (LREE) relative to chondrite. All have a significant negative Eu anomaly and nearly flat heavy REE (HREE) profiles. The mafic part of the bimodal series ranges between 39 and 58 wt.% SiO_2 , with most rocks falling within the 48 and 58 wt.% silica range. Major elements MgO , Fe_2O_{3T} , CaO and trace elements Ni, Cr, and Co show inverse relationships with silica. The mafic rocks show broad variation in Sr, Sc, V, Cr, and Ni. Like the felsic suite, the mafic rocks display broad but overlapping ranges in compatible–incompatible trace element ratios and a narrow range in REE concentrations and patterns showing enrichment in LREE relative to chondrite and nearly flat HREE profiles. Unlike the felsic suite, the mafic rocks lack a negative Eu anomaly, with the exception of one plagioclase cumulate sample that shows a positive Eu anomaly.

The mafic and felsic rocks show within-plate tectonic geochemical characteristics (Fig. 17). For the mafic rocks, enrichment in Rb, Ba, and Th and flat Ta to P and Zr to Sm profiles are similar to those of known within-plate basalts. The felsic volcanic and plutonic rocks overlap the fields of

Fig. 14. Plot of alkali oxides versus SiO_2 (in wt.%) comparing magma compositions represented in the Zarembo Island volcanic suite and in the Deer Island – Etolin Island intrusive complex. Discrimination style from LeBas et al. (1986). Rocks from the Zarembo Island – Burnett Inlet volcanic–plutonic complex define a generally bimodal suite with a gap in silica concentrations at 60–65 wt.%.

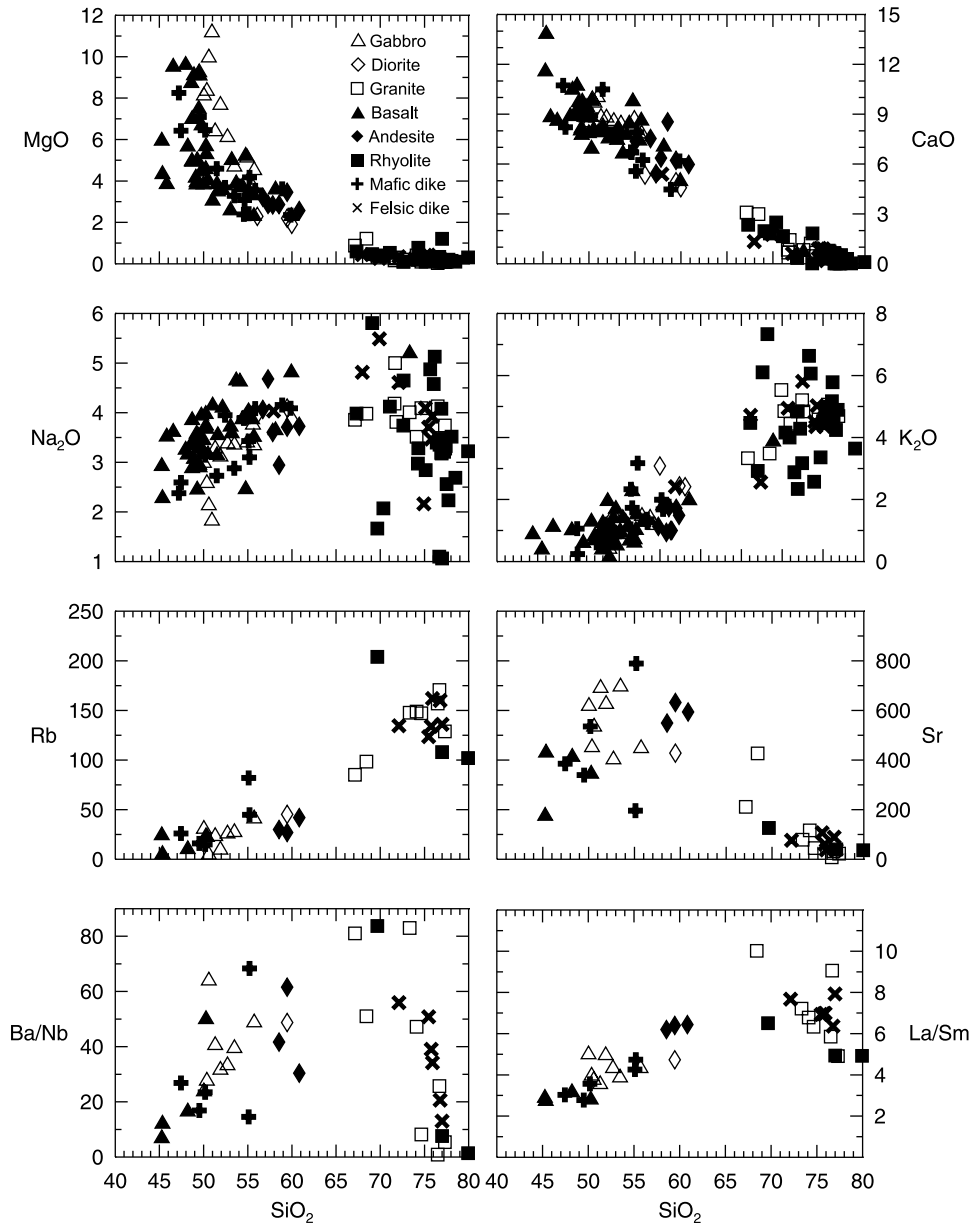


within-plate granite (WPG) and volcanic-arc granite (VAG). The VAG chemical character is likely inherited from source rocks (Gravina–Nutzotin belt rocks, mid-Cretaceous granitoids) that were generated in a volcanic-arc environment.

Discussion

Magma mingling and mixing

Isolated mafic magmatic enclaves within granite, rhyolite, and felsic dikes evidence magma mingling in both the plutonic and volcanic systems. Magma mixing is interpreted based on the ubiquitous quartz ovoids noted in many of the mafic rocks. The quartz in the andesite flows, mafic enclaves, and basalt dikes is anhedral and typically rimmed by hornblende or pyroxene. Quartz with such rims is typically explained as xenocrystic, originating in a felsic liquid. It is thought that as mafic and felsic magmas mix, quartz crystals from the felsic liquid become partially dissolved and serve as substrates for the nucleation and precipitation of mafic minerals in the new hybrid melt (Hibbard 1981; Vernon 1983, 1984, 1990). The interlayered gabbro and granite appear to record mafic replenishment events widely inferred from the study of silicic eruptive systems. Wiebe (1993a, 1993b) has proposed a general model for the evolution of a composite magma chamber by the repeated injection of basaltic liquids into a flooded silicic magma chamber resulting in mafic and silicic layered intrusions (MASLI). Wiebe (1993a) established criteria for recognizing basalt additions in flooded silicic magma chambers including (1) basally chilled gabbroic layers with lobate bases similar to sedimentary load cast structures resting on silicic layers and (2) pipes, diapirs, or veins of silicic material extending upward into basally chilled gabbroic layers; and (3) layers of broadly intermediate composition with variably assimilated mafic enclaves. Relationships in the Burnett Inlet intrusive complex indicate that mafic magma intruded into a flooded silicic magma chamber, ponded in some instances, and was

Fig. 15. Selected major and trace element variation diagrams for comparing volcanic and plutonic rock and dike compositions.

disaggregated in others. The sheeted gabbro represents new infusions into the magma chamber. The load casts, ball and pillow structures, and felsic veins at gabbro–granite interfaces clearly indicate that the mafic sheets represent a series of basaltic injections that intruded a silicic magma chamber and variably interacted with overlying granite magma and underlying crystal mush because of density contrasts between the mafic and felsic magmas (Wiebe 1974, 1993a, 1993b; Wiebe and Collins 1998; Frey 1999). In particular, the load casts, balls, and pillows formed from loading of the mafic material over a hydroplastic and unstable silicic mush. Balling and pillowing of the gabbro occurred by foundering and breakup of the semiconsolidated mafic material owing to deformation of the underlying granite, as in sedimentary analogues (Kuenen 1958). While some of the mafic material remained intact, many of the discrete pillow-form enclaves throughout the granite and alkali granite represent mafic

material that broke away from a new basaltic infusion and sank into the underlying granite. Density inversion caused diapiric upwelling of the underlying light crystal-rich silicic mush into the rapidly solidifying denser basaltic replenishment producing the dikes and veins of felsic material that project into the gabbroic layers. Overturning and mixing (Gamble 1979) caused the mineralogical and compositional heterogeneities throughout the complex, as well as the quartz ovoids noted in the andesite, mafic dikes, and enclaves and the departure of many compatible elements from coherent trends on element variation diagrams.

Genetic relationship

Because the Rb–Sr isochron on the Burnett Inlet plutonic rocks and the ages on most of the volcanic rocks are indistinguishable, we interpret the intrusive and extrusive rocks as coeval. We further interpret that the Zarembo Island volcanic

Table 1. Whole-rock geochemistry for representative rocks from the Zarembo Island volcanic suite and the Burnett Inlet plutonic complex,

Sample:	87WAC145	92JL21-1	92JL27	92JL36	92JL53	99JL86	92JL39	92JL44	92JL48	92JL55
Location:	DI	DI	EI	EI	EI	EI	EI	EI	EI	EI
Rock:	gabbro	gabbro	diorite	gabbro	gabbro	alk granite	granite	granite	granite	alk granite
SiO ₂ (wt.%)	48.80	50.80	57.40	51.40	49.60	76.22	68.47	74.45	75.60	76.90
TiO ₂	0.56	1.16	1.45	1.30	1.33	0.12	0.44	0.20	0.08	0.10
Al ₂ O ₃	15.40	16.50	15.40	17.30	16.50	12.04	16.36	12.92	12.6	12.10
Fe ₂ O _{3T}	10.00	8.84	8.40	8.83	9.66	1.99	3.05	2.70	1.14	1.66
MgO	9.59	5.88	2.12	4.50	6.17	0.03	1.21	0.10	0.09	0.09
MnO	0.16	0.15	0.13	0.13	0.14	0.03	0.07	0.04	0.01	0.01
CaO	9.33	8.26	4.76	8.08	8.52	0.32	2.99	0.66	0.55	0.18
Na ₂ O	2.05	3.25	3.95	3.22	3.16	4.11	3.98	4.08	3.44	3.72
K ₂ O	0.40	1.27	2.44	0.98	1.19	4.73	3.48	4.58	5.06	4.69
P ₂ O ₅	0.14	0.27	0.48	0.35	0.39	0.03	N/A	N/A	0.01	0.01
LOI	0.90	1.70	1.35	1.30	1.10	0.56	0.20	0.31	0.25	0.40
SUM	97.33	98.08	97.88	97.39	97.76	100.18	100.25	100.04	98.83	99.86
Sc (ppm)	N/A	17	16	N/A	16	1	N/A	N/A	N/A	13
V	310	158	141	202	154	<1	42	7	3	9
Cr	344	109	17	70	153	<1	9	9	3	0
Co	30	28	11	25	28	1	6	1	1	1
Ni	93	43	13	36	45	<1	16	17	5	1
Cu	63	65	79	108	66	<1	51	97	26	43
Zn	3	8	1	68	19	<1	5	31	23	<1
Rb	4	26	45	27	23	157	98	147	171	129
Sr	533	401	428	695	689	8	427	45	32	23
Y	11	24	38	21	22	80	15	62	29	66
Zr	43	118	247	95	110	392	110	455	173	211
Nb	3.1	10.5	21.4	9.9	13.7	39.1	15.6	46.0	13.1	28.2
Cs	0.2	1.8	2.1	2.0	2.6	2.4	3.1	2.8	4.7	2.5
Ba	201	348	1043	390	555	33	797	375	337	151
Hf	0.9	2.7	5.5	2.9	2.6	12.2	3.3	13.2	6.4	6.8
Ta	0.2	0.6	1.1	0.5	0.7	2.9	1.1	3.0	1.2	1.6
Th	0.9	3.1	5.4	2.4	2.3	21.6	14.0	20.8	27.5	16.3
U	0.3	1.2	2.2	1.2	0.9	8.0	7.3	5.8	6.4	5.6
La	7.1	18.2	36.6	16.2	17.9	68.5	35.5	57.9	48.2	38.0
Ce	15.0	33.2	67.6	30.0	36.6	132.0	54.8	99.7	75.8	81.9
Pr	1.9	4.6	9.8	3.9	5.5	15.5	5.7	11.3	8	9.5
Nd	8.8	21.3	42.4	17.1	26.2	55.7	20.2	42.8	27.3	37.9
Sm	1.89	4.22	7.75	4.21	5.07	11.70	3.55	9.14	5.32	7.75
Eu	1.14	1.17	1.74	1.45	1.60	0.15	0.83	0.39	0.25	0.30
Gd	2.14	4.62	8.06	3.92	5.11	11.90	2.97	8.79	4.53	8.68
Tb	0.34	0.71	1.16	0.58	0.72	2.15	0.41	1.40	0.67	1.64
Dy	1.94	3.93	6.25	3.68	3.77	13.30	2.52	9.09	4.3	10.43
Ho	0.39	0.71	1.12	0.76	0.67	2.83	0.49	1.94	0.92	2.02
Er	1.10	2.30	3.51	2.01	2.08	8.79	1.44	5.57	2.7	6.51
Tm	0.153	0.343	0.545	0.292	0.301	1.370	0.219	0.882	0.438	1.052
Yb	0.98	2.21	3.33	1.93	1.88	8.91	1.53	6.07	3.03	6.06
Lu	0.159	0.349	0.538	0.300	0.301	1.220	0.240	0.976	0.509	0.926

Note: DI, Deer Island; EI, Etolin Island; ZI, Zarembo Island; N/A, not analyzed.

suite and the Burnett Inlet plutonic complex are cogenetic based on the many similarities in field and geochemical characteristics described earlier in the text. Specifically, the volcanic and plutonic rocks share abundant magma mingling and mixing textures, a gap in silica at 60–65 wt.%, and major, trace, and rare-earth element compositional variations. The conspicuously bimodal character of and the igneous layering within both the volcanic and plutonic suites support a model

involving eruptive tapping of the layered granite–gabbro intrusive complex to produce the bimodal Zarembo Island volcanic suite.

The rhyolite, andesite, and basalt flows represent intermittent tapping of mafic and felsic magma chambers. The succession of basalt flows over pyroclastic layers is interpreted as early explosive eruptions of rhyolite followed by basalt effusions. The hypersolvus character of the alkali granite compared to

southeastern Alaska.

92JL1MD	92JL12MD	99JL55MD	99JL77MD	87WAC150FD	87WAC157FD	99JL55FD	99JL77FD	99JL47A	99JL55A	99JL75A
DI	DI	ZI	ZI	EI	DI	ZI	ZI	ZI	ZI	ZI
mafic dike	mafic dike	mafic dike	mafic dike	felsic dike	felsic dike	felsic dike	felsic dike	rhyolite	rhyolite	rhyolite
55.40	48.40	47.24	52.28	73.98	70.74	75.40	75.17	68.19	74.71	78.93
1.60	1.60	1.59	1.86	0.20	0.20	0.13	0.12	0.38	0.14	0.12
17.77	16.10	15.68	13.98	12.72	14.20	12.14	12.66	15.47	13.69	10.52
8.51	11.10	10.88	10.72	1.67	2.51	1.35	1.46	2.59	2.43	1.89
4.19	6.22	6.76	2.29	0.41	0.33	0.25	0.14	0.39	1.17	0.30
0.15	0.17	0.20	0.18	0.02	0.04	0.02	0.02	0.04	0.04	0.03
7.93	8.62	8.92	5.28	0.88	0.60	0.58	0.34	1.78	0.42	0.10
3.11	3.03	3.10	3.25	3.63	4.52	3.32	3.32	1.63	1.03	3.18
1.68	0.81	0.64	3.17	4.51	4.94	4.99	4.36	7.33	3.36	3.64
N/A	0.39	0.39	1.84	N/A	N/A	0.03	0.03	0.07	0.03	0.02
1.37	1.25	5.08	5.49	0.45	0.45	1.10	1.2	2.60	3.49	0.89
101.71	97.69	100.47	100.34	98.47	98.53	99.31	98.83	100.47	100.51	99.62
N/A	N/A	34	19	N/A	N/A	3	2	8	2	1
197	222	264	83	10	4	9	8	15	5	<1
14	69	137	<1	23	40	<1	<1	<1	<1	<1
26	33	40	17	4	1	2	1	2	1	<1
12	28	55	15	44	20	<1	<1	<1	<1	<1
123	111	25	16	29	42	12	<1	<1	<1	11
122	25	70	131	90	592	64	<1	<1	137	38
45	15	16	82	123	135	160	136	204	108	102
789	535	339	196	107	76	89	39	126	40	37
24	30	28	68	24	30	42	34	47	69	69
139	135	117	499	116	248	139	170	366	542	544
16.0	14.1	10.5	44.8	12.0	18.6	14.7	22.7	19.7	46.0	39.4
3.0	0.5	1.8	1.6	1.8	2.7	1.5	0.9	3.3	2.2	0.5
1094	331	177	652	610	1038	303	295	1649	350	53
4.0	3.7	3.1	10.9	4.6	7.4	5.1	5.4	9.4	14.4	13.8
0.9	0.8	0.6	2.6	1.4	1.3	1.5	2.1	1.7	3.2	2.5
4.4	2.0	1.4	7.3	14.0	16.5	19.1	19.1	14.5	17.7	14.5
1.6	0.9	0.5	3.0	5.0	4.6	7.9	6.3	6.4	7.7	1.8
24.3	19.6	11.0	48.9	28.3	49.2	34.9	40.9	48.9	41.2	39.1
42.6	37.8	24.6	102.0	45.2	80.3	66.8	74.5	90.5	89.8	131.0
5.2	5.1	3.4	13.1	5.1	8.8	7.7	8.1	10.3	10.4	9.4
21.2	21.7	15.2	52.9	18.2	31.2	26.5	27.1	36.9	37.5	35.5
5.13	5.51	3.97	11.50	4.09	6.42	5.49	5.16	7.52	8.35	7.95
1.69	1.74	1.62	3.40	0.49	0.73	0.33	0.27	1.15	0.39	0.26
4.48	5.00	4.65	12.50	3.62	5.33	5.80	5.23	7.51	10.40	8.99
0.65	0.74	0.82	2.05	0.55	0.79	1.04	0.90	1.28	1.95	1.77
4.03	4.66	4.86	11.60	3.62	4.92	6.74	5.53	7.58	11.90	11.20
0.80	0.97	1.02	2.42	0.76	1.05	1.48	1.19	1.63	2.44	2.45
2.22	2.66	2.98	7.05	2.29	2.97	4.67	3.78	4.90	7.39	7.63
0.310	0.376	0.414	1.000	0.361	0.470	0.744	0.588	0.738	1.120	1.210
2.12	2.55	2.64	6.33	2.54	3.30	5.07	3.92	5.03	7.38	8.33
0.330	0.391	0.379	0.904	0.408	0.523	0.698	0.550	0.726	1.050	1.130

the granite is consistent with crystallization under relatively low water pressures (Tuttle and Bowen 1958), which likely resulted from a release of volatiles following eruption of the volcanic edifice. Though radiometric ages are not available for the dikes, the numerous mafic and felsic dikes throughout the study are also thought to be genetically related to the volcanic–plutonic complex. The felsic dikes show magma mingling and mixing textures and both the felsic and mafic

dikes share geochemical characteristics with the volcanic and plutonic rocks. The dikes are likely feeders to higher level volcanic rocks exposed to the northwest on Kuiu Island. The extensive lahars suggest a Middle Tertiary landscape comprising steep slopes along which running water eroded, transported, and deposited large volcanic debris flows. We conceptualize that the original volcanic–plutonic structure consisted of volcanic rocks at the highest levels underlain by alkali granite and

Table 1 (concluded).

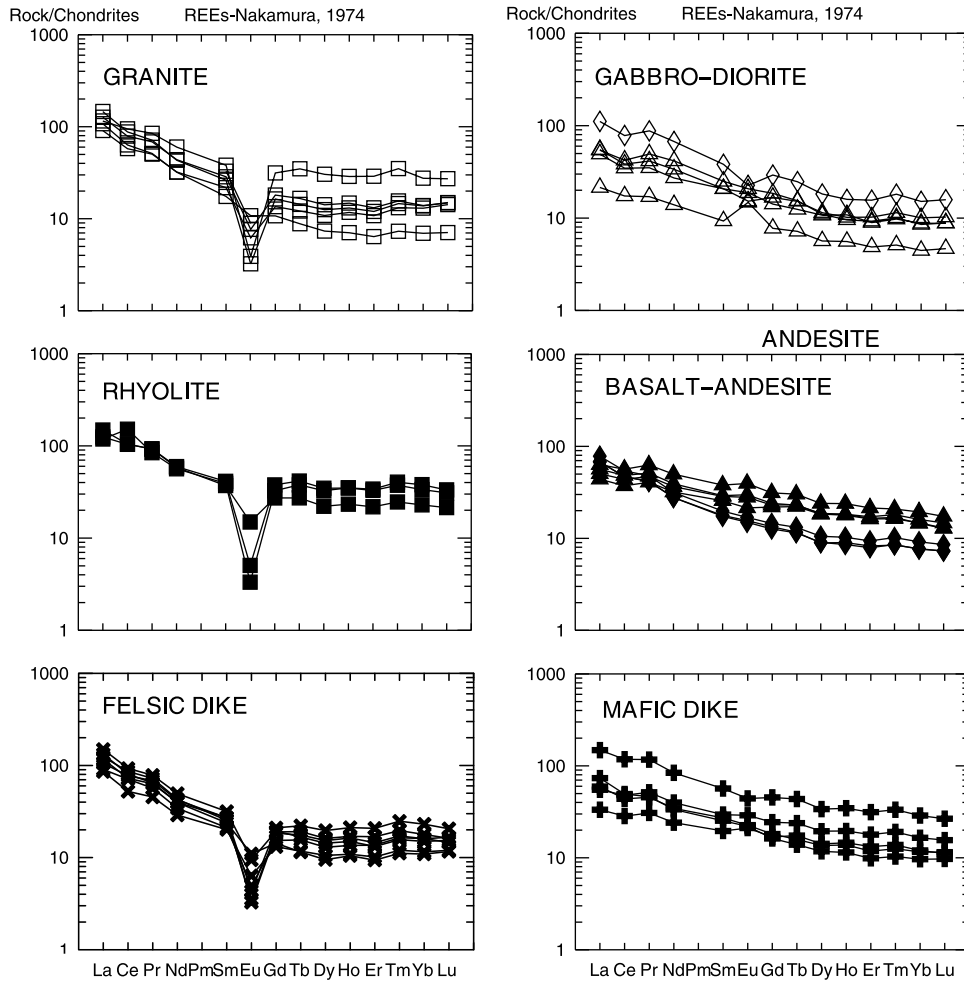
Sample:	99JL47C	99JL54B	99JL54C	99JL56B	99JL59C	99JL75B
Location:	ZI	ZI	ZI	ZI	ZI	ZI
Rock:	basalt	andesite	andesite	andesite	basalt	basalt
SiO ₂ (wt.%)	47.95	56.45	56.33	57.35	40.53	46.99
TiO ₂	1.98	0.80	0.82	0.86	2.99	2.46
Al ₂ O ₃	15.53	17.34	17.32	17.16	13.71	15.96
Fe ₂ O _{3T}	12.87	6.23	6.45	5.39	12.58	11.66
MgO	5.40	3.28	2.75	2.42	3.86	5.5
MnO	0.19	0.11	0.10	0.11	0.24	0.17
CaO	6.58	5.90	8.21	5.63	12.34	10.19
Na ₂ O	3.56	3.52	2.83	3.51	2.03	3.07
K ₂ O	0.94	1.00	1.00	1.49	0.38	0.68
P ₂ O ₅	0.35	0.30	0.39	0.34	0.70	0.78
LOI	4.86	4.39	4.64	4.98	9.28	2.76
SUM	100.22	99.32	100.84	99.23	98.64	100.22
Sc (ppm)	34	13	13	13	38	34
V	267	97	110	108	328	282
Cr	122	46	53	47	80	153
Co	46	5	18	13	28	42
Ni	54	<1	48	156	44	78
Cu	26	14	32	23	36	46
Zn	165	<1	80	55	68	94
Rb	23	27	30	42	5	10
Sr	344	632	549	594	429	412
Y	37	14	19	22	45	36
Zr	164	134	152	172	160	181
Nb	12.7	8.6	13.9	15.1	22.4	20.5
Cs	1.2	1.3	1.3	3.9	1.8	2.1
Ba	633	529	579	459	268	336
Hf	4.4	3.4	3.5	4.1	4.6	4.5
Ta	0.8	0.8	0.8	1.0	1.3	1.2
Th	2.0	3.7	3.8	4.6	0.9	1.2
U	0.9	1.7	1.6	2.0	0.4	0.5
La	14.5	22.5	22.3	25.8	20.9	18.6
Ce	32.2	40.5	40.4	46.9	48.8	41.7
Pr	4.6	4.6	4.7	5.4	7.0	5.8
Nd	20.1	17.5	17.5	19.9	31.4	24.7
Sm	5.20	3.52	3.60	4.01	7.69	5.91
Eu	1.65	1.15	1.20	1.30	3.04	2.29
Gd	6.04	3.49	3.69	4.00	8.61	6.62
Tb	1.04	0.54	0.55	0.62	1.42	1.08
Dy	6.27	3.10	3.07	3.61	8.22	6.4
Ho	1.28	0.60	0.63	0.72	1.67	1.28
Er	3.86	1.78	1.86	2.11	4.81	3.7
Tm	0.543	0.257	0.254	0.306	0.625	0.506
Yb	3.53	1.68	1.70	2.02	4.26	3.20
Lu	0.499	0.248	0.247	0.291	0.589	0.436

granite at intermediate levels with gabbro-diorite at the base of the complex. Thus, the continuous exposure of plutonic and volcanic rocks along a northwest–southeast transect suggests that the Zarembo Island – Burnett Inlet volcanic–plutonic complex is preserved within a crustal block that has been tilted at least 7° to the northwest, based on emplacement depths of ~8 km for the gabbro at the southeast end of the complex. This conclusion is in agreement with other models for the region invoking east side up tilting (Cook and Crawford 1994; Butler et al. 2001).

Tectonic setting

The lack of continuous trends from the mafic to the felsic suite on element–element diagrams indicates that the volcanic and plutonic rocks did not evolve through differentiation of a single mafic magma. Rather, disparate mafic and felsic lavas were involved in the generation and evolution of both the volcanic and plutonic suites. The within-plate geochemical characteristics of the volcanic and plutonic rocks studied here and the distinctly bimodal nature of magmatism favors an origin in a crustal extension environment.

Fig. 16. Rare-earth element abundances in samples compared to those of chondrites (normalization factors of Nakamura 1974). Volcanic, plutonic, and dike rocks within the felsic group and mafic group have nearly identical chondrite-normalized REE patterns.



Bimodal magmatism is commonly associated with continental rift settings, like the Basin and Range Province of the western United States, in which extension-induced mantle melting produces basalts that easily erupt in an extensional stress regime while generating anatectic rhyolite magmas from continental crust and/or basalt emplaced earlier in the crust. Subsequent mafic infusions into dominantly felsic magma chambers may induce silicic explosive eruptions (Sparks et al. 1977; Koyaguchi and Blake 1989; Koyaguchi 1991; Huppert and Sparks 1988). The sequence of explosive volcanic rocks followed by basalt flows within the Zarembo Island volcanic stratigraphy supports such a model.

Evidence for deformation

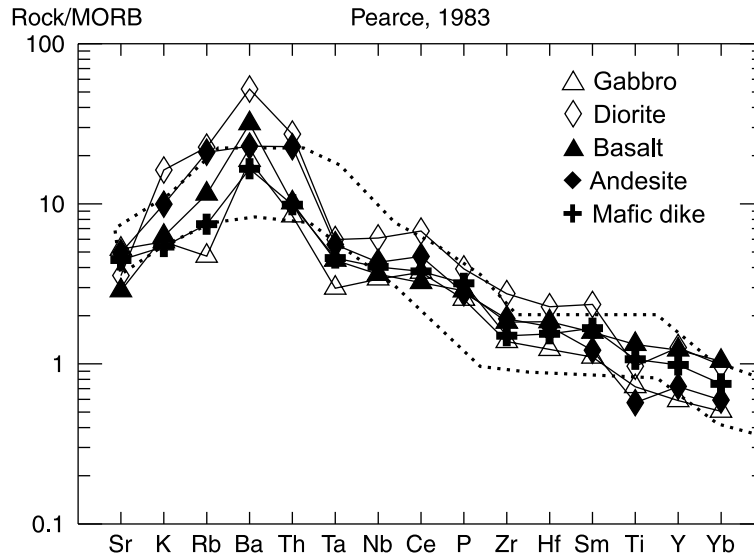
Magmatic reorientation

Unlike well-studied MASLI in the Coastal Maine Magmatic Province (Wiebe 1993a, 1993b; Frey 1999) and the Sierra Nevada batholith (Wiebe et al. 2002), the Burnett Inlet gabbro–granite complex lacks indisputable silicic pipes, whose orientations are typically taken as an approximate measure of vertical at the time of deposition (Chapman and Rhodes 1992; Wiebe and Collins 1998). Also, limited exposures of the gabbro–diorite prevent a comprehensive study of the three-dimensional geometry of the plutonic layers, the frequency

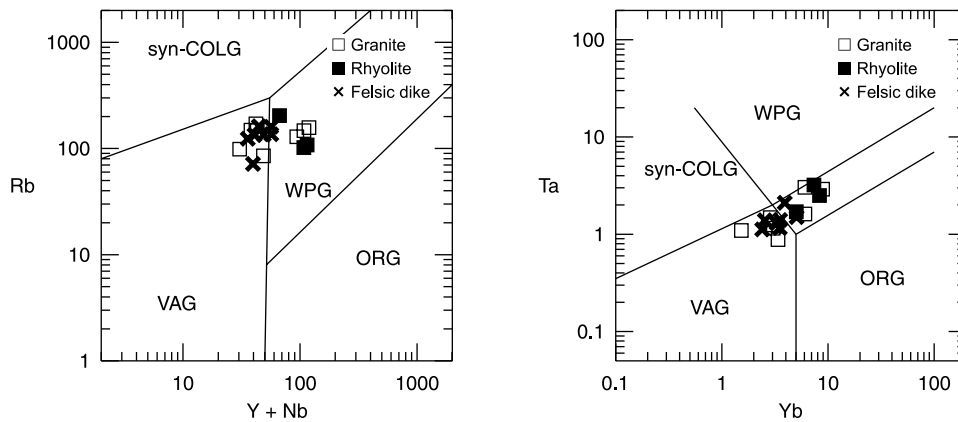
of mafic–felsic alternations, and the mineralogical and grain-size variations within any one layer. Though most of the plutonic stratiform depositional features dip to the northwest, there are some that deviate from this trend (Fig. 2). It is possible that (i) the region experienced post-20 Ma deformation; (ii) the floor of the magma chamber was not horizontal when the mafic magma flowed across it (Wiebe et al. 2002); or (iii) synmagmatic disturbances disrupted the igneous layering. We have already established, based on the continuous exposure of the plutonic and volcanic rocks, that the herein proposed volcanic–plutonic complex sits within a crustal block that has been tilted to the northwest. The variable orientation of volcanic layering (Fig. 2) may be the result of tilting of smaller crustal segments. Though it is impossible to know the original attitude of the magma chamber floor, it is clear that the plutonic layering was disrupted in the magmatic state. Recall that all of the mafic rafts in Fig. 7 have one flat, smooth side and another flat but crenulated side. These characteristics are similar to undisturbed mafic sheets in a MASLI located on Vinalhaven Island, Maine that are systematically flat-topped with wispy veins of granite along the base (Frey 1999). Just like silicic pipes, the orientation of the felsic veins can be used to determine “up” direction in a relatively undisturbed body (Wiebe 1993a, 1993b). We interpret the randomly oriented mafic rafts in Fig. 7 as frag-

Fig. 17. (A) Comparison of trace element content in mafic rock samples compared with those of normal mid-ocean ridge basalt (MORB). Diagram after Pearce (1983). Normalization factors of Sun and McDonough (1989). Dashed envelope shows area encompassing compositions of known within-plate basalts from Antarctica (Kyle 1981) and Ethiopia (Brotzu et al. 1981). (B) Plot of felsic rocks after Pearce et al. (1984). Syn-COLG, syn-collision granite; WPG, within-plate granite; VAG, volcanic-arc granite; ORG, ocean-ridge granite. Samples plot within the fields of volcanic-arc and within-plate granites.

A MAFIC ROCKS



B FELSIC ROCKS



ments of tabular sheets of gabbro that intruded into lower areas of the granite chamber and were subsequently disrupted by convective circulation in the granitic magma in response to mafic injections. The crenulated side of these rafts was the base of the sheet, while the smooth side was the top of the sheet that is now upside down.

Brittle deformation

Rocks in the study area were affected by post-20 Ma transtension, as evidenced by numerous faults and dikes that occur throughout the region. Northwest-southeast and north-south strike-slip faults locally cut portions of the Burnett Inlet granite-gabbro complex along Canoe Passage, Burnett Inlet, and Steamer Bay (Karl et al. 1999; Koch et al. 1977). The mafic and felsic dikes that intrude the volcanic-plutonic complex show a preferred northeast-southwest strike and a subordinate

northwest-southeast strike (Fig. 2a). As dikes propagate perpendicular to the direction of extension, the two dike sets record major planes of crustal extension and magma intrusion. The tectonic plate reconstructions of Stock and Molnar (1988) indicate that between 10 and 20 Ma, the Pacific Plate was colliding with western North America at a highly oblique angle. The stress ellipse in Fig. 2b shows the stress fields affecting the region during the Middle Tertiary, as well as the orientation of conjugate shear fractures that develop within such a stress regime. The northeast-southwest and northwest-southeast dike sets parallel the shear fracture orientations. The greater number of northeast-southwest dikes relate to the plane of crustal extension caused by the northwest-southeast relative strike-slip (transform margin) motions of the Pacific and North American plates that developed during the Late Eocene and Miocene (Engebretson et al. 1985; Stock and

Molnar 1988; Lonsdale 1988) and have dominated the region since 10 Ma.

Implications

Our geological, geochemical, and structural lines of evidence lead us to conclude that the Zarembo Island – Burnett Inlet volcanic–plutonic complex originated in an extensional setting and experienced post-20 block faulting and tilting. These results have important implications for understanding the geologic evolution of the northern portion of the Northern American Cordillera and resolving the Baja British Columbia debate. The Baja British Columbia hypothesis proposes that the Insular superterrane and Coast Mountains orogen were located 3000–4000 km to the south during mid-Cretaceous time (Cowan et al. 1997). This is based primarily on discordant paleomagnetic poles in intrusions of mid-Cretaceous age. The paleomagnetic data can be explained by assuming systematic tilting down to the southwest, by translation of > 2000 km from the south, or some combination of the two. Available paleomagnetic evidence in the Prince Rupert (Butler et al. 2001, 2002) and Queen Charlotte (Irving et al. 1992) regions favors a tilt plus moderate (~1000 km) northward translation model rather than the Baja British Columbia model (Vandall 1993). This study suggests that crustal tilting has occurred as far north as central southeastern Alaska after the Middle Miocene. Establishing the timing and magnitude of post-Cretaceous tilting in this region will provide crucial information for paleomagnetic studies aimed at resolving the mid-Cretaceous paleogeography of the western margin of North America.

Conclusions

The Zarembo Island volcanic rocks are the eruptive products of the Burnett Inlet granite–gabbro intrusive complex. The volcanic–plutonic system developed through repeated mafic magma injections into a floored silicic magma chamber that originated through partial crustal melting triggered by basalt emplacement during lithosphere extension and thinning. The associated volcanic rocks provide evidence that this was a shallow-crustal subvolcanic magma chamber. Outcrops near the base of the complex reveal evidence for plutonic layering and thus provide another example of a granite–gabbro complex that evolved through periodic injections of basalt into a silicic magma chamber. Density and thermal instabilities related to felsic–mafic magmatic successions caused episodic volcanic eruptions and disturbed the orientation of the magmatic layers. Following eruption of the system at about 20 Ma, the complex was tilted to the northwest during regional crustal extension. The correlation of the Zarembo Island volcanic rocks and the Burnett Inlet intrusive complex opens the possibility that other bimodal plutonic and volcanic rocks in the Kuiu–Etolin magmatic province, such as the diorite–granite on central Kuiu Island and the basalt–rhyolite on Kupreanof Island, are related and that the province represents a major Middle to Upper Tertiary domain of crustal extension, as first suggested by Brew (1994).

Acknowledgments

This research was funded by National Science Foundation

grant EAR-9526344, part of the Continental Dynamics ACCRETE Project, with Principal Investigators Lincoln Hollister and Maria Luisa Crawford. The New Mexico Highlands University Faculty Research Funds provided additional financial support to J. Lindline. We thank Captain Rick Mathews for his assistance in field operations. John Greenough, Peter Reiners, and Robert Wiebe provided very helpful reviews.

References

- Bacon, C.R. 1986. Magmatic inclusions in silicic and intermediate volcanic rocks. *Journal of Geophysical Research*, **91**: 6091–6112.
- Bacon, C.R., and Metz, J. 1984. Magmatic inclusions in rhyolites, contaminated basalts, and compositional zonation beneath the Coso volcanic field, California. *Contributions to Mineralogy and Petrology*, **85**: 346–365.
- Berg, H.C., Jones, D.L., and Richter, D.H. 1972. Gravina–Nutzotin Belt — tectonic significance of an upper Mesozoic sedimentary and volcanic sequence in southern and southeastern Alaska. United States Geological Survey, Professional Paper 800D, pp. D1–D24.
- Brew, D.A. 1994. Latest Mesozoic and Cenozoic magmatism in southeastern Alaska. *In The Geology of Alaska. Edited by G. Plafker and H.C. Berg. The Geology of North America, Geological Society of America, Boulder, Colo., Vol. G., pp. 621–656.*
- Brew, D.A., and Morrell, R.P. 1983. Intrusive rocks and plutonic belts in southeastern Alaska, U.S.A. *In Circum-Pacific plutonic terranes. Edited by J.A. Roddick. Geological Society of America, Memoir 159, pp. 171–193.*
- Brew, D.A., Berg, H.C., Morrell, R.P., Sonnevil, R.S., Hunt, S.J., and Huie, C. 1979. The mid-Tertiary Kuiu–Etolin volcanic–plutonic belt, southeastern Alaska. *In The United States Geologic Survey in Alaska: accomplishments during 1978. Edited by K.M. Johnson and J.R. Williams. United States Geological Survey, Circular 804-B, pp. B129–B130.*
- Brew, D.A., Sonnevil, R.A., Hunt, S.J., and Ford, A.B. 1981. Newly recognized alkali granite stock, southwestern Kupreanof Island, Alaska. *In The United States Geologic Survey in Alaska: accomplishments during 1979. Edited by N.R.D. Albert and T. Hudson. United States Geological Survey, Circular 823-B, pp. B108–B109.*
- Brew, D.A., Ovenshine, A.T., Karl, S.M., and Hunt, S.J. 1984. Preliminary reconnaissance geologic map of the Petersburg and parts of the Port Alexander and Sumdum 1 : 250 000 quadrangles, southeastern Alaska. United States Geological Survey, Open-file Report 84-405.
- Brotzu, P., Ganzerli-Valentini, M.T., Morbidelli, L., Piccirillo, E.M., Stella, R., and Traversa, G. 1981. Basaltic volcanism in the Northern sector of the main Ethiopian rift. *Journal of Volcanological Research*, **10**: 365–382.
- Butler, R.F., Gehrels, G.E., Crawford, M.L., and Crawford, W.A. 2001. Paleomagnetism of the Quottoon plutonic complex in the Coast Mountains of British Columbia and southeastern Alaska: Evidence for tilting during uplift. *Canadian Journal of Earth Sciences*, **38**: 1367–1384.
- Butler, R.F., Gehrels, G.E., Baldwin, S.L., and Davidson, C. 2002. Paleomagnetism and geochronology of the Ecstall pluton in the Coast Mountains of British Columbia: Evidence for local deformation rather than large-scale transport. *Journal of Geophysical Research*, **107**: 3-1 – 3-13.
- Chapman, M., and Rhodes, J.M. 1992. Composite layering in the Isle au Haut Igneous Complex, Maine: Evidence for periodic

- invasion of a mafic magma into an evolving magma reservoir. *Journal of Volcanology and Geothermal Research*, **51**: 41–60.
- Coney, P.J., and Jones, D.L. 1985. Accretion tectonics and crustal structure in Alaska. *Tectonophysics*, **119**: 265–283.
- Coney, P.J., Jones, D.L., and Monger, J.W.H. 1980. Cordilleran suspect terranes. *Nature*, **188**: 329–333.
- Cook, R.D., and Crawford, M.L. 1994. Exhumation and tilting of the western metamorphic belt of the Coast orogen in southern southeastern Alaska. *Tectonics*, **13**: 528–537.
- Cowan, D.S., Brandon, M.T., and Garver, J.I. 1997. Geologic tests of hypotheses for large coastwise displacements: A critique illustrated by the Baja British Columbia controversy. *American Journal of Science*, **297**: 167–173.
- Douglass, S.L., Webster, J.H., Burrell, P.D., Lanphere, M.L., and Brew, D.A. 1989. Major-element chemistry, radiometric ages, and locations of samples from the Petersburg and parts of the Port Alexander and Sumdum quadrangles, southeastern Alaska. United States Geological Survey, Open-file Report 89–527.
- Eichelberger, J.C. 1980. Vesiculation of mafic magma during replenishment of silicic magma reservoirs. *Nature*, **288**: 446–450.
- Engebretson, D.C., Gordon, R.G., and Cox, A. 1985. Relative motions between oceanic and continental plates in the Pacific basin. *Geological Society of America Special Paper*, 206.
- Feigenson, M.D., and Carr, M.J. 1985. Determination of major, trace and rare-earth elements by DCP-AES. *Chemical Geology*, **51**: 19–27.
- Frey, H.M. 1999. Interactions between mafic and silicic magmas in Vinalhaven granite–gabbro complex, coastal Maine. Senior Honors thesis, Franklin and Marshall College, Lancaster, Pa.
- Frost, T.P., and Mahood, G.A. 1987. Field, chemical and physical constraints on mafic–felsic magma interaction in the Lamark Granodiorite, Sierra Nevada, California. *Geological Society of America Bulletin*, **99**: 272–291.
- Furman, T., and Spera, F.J. 1985. Co-mingling of acid and basic magma with implications for the origin of I-type xenoliths: field and petrochemical relations of an unusual dike complex at Eagle Lake, Sequoia National Park, California, USA. *Journal of Volcanology and Geothermal Research*, **24**: 151–178.
- Gamble, J.A. 1979. The geochemistry and petrogenesis of dolerites and gabbros from the Tertiary central volcanic complex of Slieve Gullion, northeast Ireland. *Contributions to Mineralogy and Petrology*, **69**: 5–19.
- Gehrels, G.E., McClelland, W.C., Samson, S.D., Petchett, P.J., and Brew, D.A. 1991. U–Pb geochronology of the Late Cretaceous and early Tertiary plutons in the northern Coast Mountains Batholith. *Canadian Journal of Earth Science*, **28**: 899–911.
- Gerdes, M. 1988. P–T constraints on metamorphism of metasediments in the Ketchikan and Petersburg Quadrangles, Southeast Alaska; Senior thesis, Bryn Mawr College, Bryn Mawr, Pa.
- Hibbard, M.J. 1981. The magma mixing origin of mantled feldspars. *Contributions to Mineralogy and Petrology*, **76**: 158–170.
- Hunt, S.J. 1984. Preliminary study of a zoned leucocratic-granite body on central Etolin Island, southeastern Alaska. *In The United States Geological Survey in Alaska: accomplishments during 1981*. Edited by W.L. Coonrad and R.L. Elliot. United States Geological Survey, Circular 868, pp. 128–131.
- Huppert, H.E., and Sparks, R.S.J. 1988. The generation of granitic magmas by intrusion of basalt into continental crust. *Journal of Petrology*, **29**: 599–624.
- Irvine, T.N., and Baragar, W.R.A. 1971. A guide to the chemical classification of the common volcanic rocks. *Canadian Journal of Earth Sciences*, **8**: 523–548.
- Irving, E., Souther, J.G., and Baker, J. 1992. Tertiary extension and tilting in the Queen Charlotte Islands, evidence from dyke swarms and their paleomagnetism. *Canadian Journal of Earth Sciences*, **29**: 1878–1898.
- Jones, D.L., Siberling, N.J., Bert, H.C., and Plafker, G., 1981. Tectonostratigraphic terrane map of Alaska. United States Geological Survey, Open-file Report 81-792.
- Karl, S.M., Haeussler, P.J., and McCafferty, A.E. 1999. Reconnaissance Geologic Map of the Duncan Canal/Zarembo Island Area, Southeastern Alaska. United States Geological Survey, Open-file Report 99-168.
- Koch, R.D., Smith, J.G., and Elliot, R.L. 1977. Miocene or younger strike-slip (?) fault at Canoe Passage, southeastern Alaska. *In Geological studies in Alaska by the U.S. Geological Survey during 1976*. Edited by K.M. Blean. United States Geological Survey, Circular 751-B, p. B76.
- Koyaguchi, T. 1991. Enclaves in volcanic rocks from Japan. *In Enclaves and granite petrology*. Edited by J. Didier and B. Barbarin. Elsevier, Amsterdam, The Netherlands, pp. 235–250.
- Koyaguchi, T., and Blake, S. 1989. The dynamics of magma mixing in a rising magma batch. *Bulletin of Volcanology*, **52**: 127–137.
- Kuenen, P.H. 1958. Experiments in geology. *Geological Society of Glasgow Transactions*, **23**: 1–28.
- Kyle, P.R. 1981. The mineralogy and geochemistry of a basanite to phonolite sequence at Hut Point Peninsula, Antarctica, based on ore from the Dry Valley Drilling Project drillholes 1, and 3. *Journal of Petrology*, **22**: 451–500.
- Le Bas, M.J., LeMaitre, R.W., Streicheisen, A., and Zanettin, B. 1986. A chemical classification for volcanic rocks based on the total alkali-silica diagram. *Journal of Petrology*, **27**: 745–750.
- Lindline, J., Crawford, W.A., Crawford, M.L., and Omar, G.I. 2000. Post-accretion magmatism within the Kuiu–Etolin igneous belt, southeastern Alaska. *Canadian Mineralogist*, **38**: 951–974.
- Lonsdale, P. 1988. Paleogene history of the Kula Plate: Offshore evidence and onshore implications. *Geological Society of America Bulletin*, **100**: 733–754.
- Monger, J.W.H., Price, R.A., and Tempelman-Kluit, D.J. 1982. Tectonic accretion and the origin of two major metamorphic and plutonic belts in the Canadian Cordillera. *Geology*, **10**: 70–75.
- Nakamura, N. 1974. Determination of REE, Ba, Fe, Mg, Na, and K in carbonaceous and ordinary chondrites. *Geochimica et Cosmochimica Acta*, **38**: 757–775.
- Pearce, J.A. 1983. Role of sub-continental lithosphere in magma genesis at active continental margins. *In Continental basalts and mantle xenoliths*. Edited by C.J. Hawkesworth, C.J. and M.J. Norry. Shiva Publications, Nantwich, UK, pp. 230–249.
- Pearce, J.A., Harris, N.B.W., and Tindle, A.G. 1984. Trace element discrimination diagrams for the tectonic interpretation of granitic rocks. *Journal of Petrology*, **25**: 956–983.
- Saltus, R.W., and Simmons, G.C. 1997. Composite and merged aeromagnetic data for Alaska: A website for distribution of gridded data and plot files. United States Geological Survey, Open-file Report 97-520.
- Sparks, S.R.J., Sigurdsson, H., and Wilson, L. 1977. Magma mixing: a mechanism for triggering acid explosive eruptions. *Nature*, **267**: 315–318.
- Stock, J., and Molnar, R.P. 1988. Uncertainties and implications of Late Cretaceous and Tertiary positions of the North America plate relative to the Farallon, Kula and Pacific plates. *Tectonophysics*, **7**: 465–487.
- Sun, S.-S., and McDonough, W.F. 1989. Chemical and isotopic systematics of oceanic basalt: Implications for mantle compositions and processes. *In Magmatism in the ocean basins*. Edited by A.D. Saunders and M.J. Norry. Geological Society (of London) Special Publication 42, pp. 313–345.
- Tuttle, O.F., and Bowen, N.L. 1958. Origin of granite in the light

- of experimental studies in the system $\text{NaAlSi}_3\text{O}_8\text{-SiO}_2\text{-H}_2\text{O}$: Geological Society of America, Memoir 74.
- Vandall, T.A. 1993. Cretaceous Coast Belt paleomagnetic data from the Spetch Creek pluton, B.C.: Evidence for the "tilt and moderate displacement" model. *Canadian Journal of Earth Science*, **30**: 1037–1048.
- Vernon, R.H. 1983. Restite, xenoliths, and microgranitoid enclaves in granites. *Journal of the Proceedings Royal Society of New South Wales*, **116**: 77–103.
- Vernon, R.H. 1984. Microgranitoid enclaves: globules of hybrid magma quenched in a plutonic environment. *Nature*, **304**: 438–439.
- Vernon, R.H. 1990. Crystallization and hybridism in microgranitoid enclave magmas: microstructural evidence. *Journal of Geophysical Research*, **95**: 17 849 – 17 859.
- Wheeler, J.O., Brookfield, A.J., Gabrielses, H., Monger, J.W.H., Tipper, T.W., and Woodsworth, G.J. 1991. Terrane map of the Canadian Cordillera. Geological Survey of Canada, Map 1713A.
- Wiebe, R.A. 1974. Coexisting intermediate and basic magmas, Ingonish, Nova Scotia. *Journal of Geology*, **82**: 74–87.
- Wiebe, R.A. 1988. Structural and magmatic evolution of a magma chamber: the Newark Island layered intrusion, Nain, Labrador. *Ibid.*, **29**: 239–269.
- Wiebe, R.A. 1993a. Basaltic injections into floored silicic magma chambers. *EOS Transactions, American Geophysical Union*, **74**: 1, 3.
- Wiebe, R.A. 1993b. Pleasant Bay layered gabbro–diorite, coastal Maine: Ponding and crystallization of basaltic injections into a silicic magma chamber. *Journal of Petrology*, **44**: 461–489.
- Wiebe, R.A., and Collins, W.J. 1998. Depositional features and stratigraphic sections in granitic plutons: Implications for the emplacement and crystallization of granitic magma. *Journal of Structural Geology*, **20**: 1273–1289.
- Wiebe, R.A., Blair, K.D., Hawkins, D.P., and Sabine, C.P. 2002. Mafic injections, in situ hybridization, and crystal accumulation in the Pyramid Peak granite, California. *Geological Survey of America Bulletin*, **114**: 909–920.
- Zorpi, M.J., Coulin, C., Orsini, J.B., and Cocirca, C. 1989. Magma mingling, zoning and emplacement in calc-alkaline granitoid plutons. *Tectonophysics*, **157**: 315–329.